Vector field tomography: overcoming the ill posedness of the problem

Alexandra Koulouri
Supervisor: Maria Petrou

Imperial College London

12/1/2011

Vector field tomography

The methods and algorithms for tomographic reconstruction of vector fields when having integral information.

Vector field tomography

The methods and algorithms for tomographic reconstruction of vector fields when having integral information.

Definition (Vectorial ray transform-VRT)

Line integral:

$$I_L = \int_L \mathbf{F} \cdot d\mathbf{r} = \int \mathbf{F} \cdot \hat{\mathbf{r}} dr$$

where $\hat{\mathbf{r}}$ is the unit vector in the direction of line L and $\mathbf{F}$ is the vector field to be recovered.

Vector field tomography

The methods and algorithms for tomographic reconstruction of vector fields when having integral information.

Definition (Vectorial ray transform-VRT)

Line integral:

$$I_L = \int_L \mathbf{F} \cdot d\mathbf{r} = \int \mathbf{F} \cdot \hat{\mathbf{r}} dr$$

where $\hat{\mathbf{r}}$ is the unit vector in the direction of line L and $\mathbf{F}$ is the vector field to be recovered.

Inverse problem$\rightarrow$ Ill posed.

Mathematical Basics

- Vector field tomographic methods employ the theory founded by Radon for the scalar problem.

Mathematical Basics

- Vector field tomographic methods employ the theory founded by Radon for the scalar problem.
- The recovery of a scalar functions $f(x, y)$ from line integral applying the Central Slice Theorem(CST) is a well known problem.

Mathematical Basics

- Vector field tomographic methods employ the theory founded by Radon for the scalar problem.
- The recovery of a scalar functions $f(x, y)$ from line integral applying the Central Slice Theorem(CST) is a well known problem.
- But vector field **F** has 2 or 3 components and therefore full recovery is impossible.

Theoretical work for vector field recovery

For the recovery of a vector field previous methods used Helmholtz decomposition theorem where vector **F** is decomposed in two components.

Theoretical work for vector field recovery

For the recovery of a vector field previous methods used Helmholtz decomposition theorem where vector **F** is decomposed in two components.

- irrotational: $\nabla\Phi$

Theoretical work for vector field recovery

For the recovery of a vector field previous methods used Helmholtz decomposition theorem where vector **F** is decomposed in two components.

- irrotational: $\nabla\Phi$
- solenoidal: $\nabla \times \mathbf{A}$

Theoretical work for vector field recovery

For the recovery of a vector field previous methods used Helmholtz decomposition theorem where vector **F** is decomposed in two components.

- irrotational: $\nabla\Phi$
- solenoidal: $\nabla \times \mathbf{A}$

Such as

$$\mathbf{F} = \nabla \times \mathbf{A} - \nabla\Phi$$

Theoretical work for vector field recovery

For the recovery of a vector field previous methods used Helmholtz decomposition theorem where vector $\mathbf{F}$ is decomposed in two components.

- irrotational: $\nabla\Phi$
- solenoidal: $\nabla \times \mathbf{A}$

Such as

$$\mathbf{F} = \nabla \times \mathbf{A} - \nabla\Phi$$

Application of CST to the vectorial ray transform results the recovery of the solenoidal component $\nabla \times \mathbf{A}$ of the vector field [Norton].

Proposed solutions for full reconstruction

As only the solenoidal component can be recovered two basic ideas were proposed:

Proposed solutions for full reconstruction

As only the solenoidal component can be recovered two basic ideas were proposed:

Proposed solutions for full reconstruction

As only the solenoidal component can be recovered two basic ideas were proposed:

- extra measurements i.e.

$$I_{\perp} = \int \mathbf{F} \cdot \hat{\mathbf{r}}_{\perp} \, dr$$

[Braun-Hauck and later Prince and Osman].

Proposed solutions for full reconstruction

As only the solenoidal component can be recovered two basic ideas were proposed:

- extra measurements i.e.

$$I_{\perp} = \int \mathbf{F} \cdot \hat{\mathbf{r}}_{\perp} \, dr$$

  [Braun-Hauck and later Prince and Osman].
  Main drawback is the difficulty of taking traversal measurements which makes the method impractical.

Proposed solutions for full reconstruction

As only the solenoidal component can be recovered two basic ideas were proposed:

- extra measurements i.e.

$$I_{\perp} = \int \mathbf{F} \cdot \hat{\mathbf{r}}_{\perp} dr$$

  [Braun-Hauck and later Prince and Osman].
  Main drawback is the difficulty of taking traversal measurements which makes the method impractical.

- Further assumptions e.g. no sources inside the field's domain [Norton].

Proposed solutions for full reconstruction

As only the solenoidal component can be recovered two basic ideas were proposed:

- extra measurements i.e.

$$I_{\perp} = \int \mathbf{F} \cdot \hat{\mathbf{r}}_{\perp} dr$$

  [Braun-Hauck and later Prince and Osman].
  Main drawback is the difficulty of taking traversal measurements which makes the method impractical.

- Further assumptions e.g. no sources inside the field's domain [Norton]. However, real problems like EEG include sources

Vector field tomographic method–Motivation

Recovery of an irrotational vector field $\mathbf{E} = -\nabla\Phi$ in a bounded homogeneous domain.

Vector field tomographic method–Motivation

Recovery of an irrotational vector field $\mathbf{E} = -\nabla\Phi$ in a bounded homogeneous domain.

Main practical application:Inverse Bioelectric Field Problem

Vector field tomographic method–Motivation

Recovery of an irrotational vector field $\mathbf{E} = -\nabla\Phi$ in a bounded homogeneous domain.

Main practical application:Inverse Bioelectric Field Problem

$$\text{Model Equation: VRT } I_{L k} = \int_{L_k} \mathbf{E} \cdot d\mathbf{r} = \Phi(\mathbf{a}) - \Phi(\mathbf{b})$$

Path Independent:Φ at starting point **a** and endpoint **b** of line L_k.

Physical Assumptions

Physical Assumptions

- Stationarity→ constant during the time of measurements.

Physical Assumptions

- Stationarity$\rightarrow$ constant during the time of measurements.
- Irrotational $\rightarrow \nabla \times \mathbf{E} = 0 \Leftrightarrow \int_{Closed-Path} \mathbf{E} dc = 0$.

Physical Assumptions

- Stationarity$\rightarrow$ constant during the time of measurements.
- Irrotational $\rightarrow \nabla \times \mathbf{E} = 0 \Leftrightarrow \int_{Closed-Path} \mathbf{E} d\mathbf{c} = 0.$
- Bandlimited

Direct numerical method

Direct numerical method

- Definition of *model equations* adapted to the physical properties.

Direct numerical method

- Definition of *model equations* adapted to the physical properties.
- Design of the geometric model where these equations operate.

Direct numerical method

- Definition of *model equations* adapted to the physical properties.
- Design of the geometric model where these equations operate.
- Discretization of the equations to form a numerical system.

Formulation based on Petrou–Giannakidis idea

$2D$ continuous square domain $\rightarrow N \times N$ grid.
Recovery of $2D$ vector field in each tile $\rightarrow 2N^2$ unknowns.

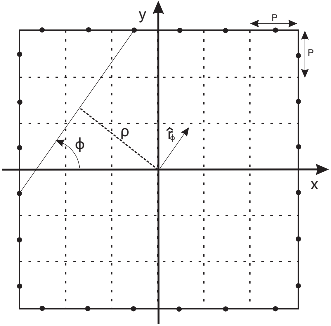

Formulation based on Petrou–Giannakidis idea

$2D$ continuous square domain $\rightarrow N \times N$ grid.
Recovery of $2D$ vector field in each tile $\rightarrow 2N^2$ unknowns.

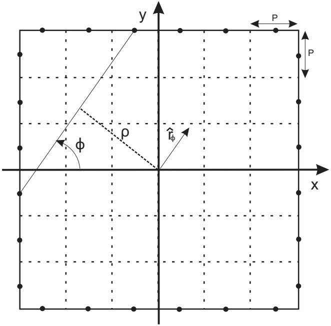

- $4N$ boundary measurements

Formulation based on Petrou–Giannakidis idea

$2D$ continuous square domain $\rightarrow N \times N$ grid.
Recovery of $2D$ vector field in each tile $\rightarrow 2N^2$ unknowns.

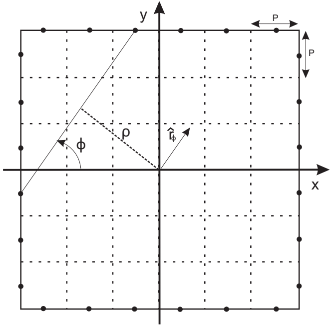

- $4N$ boundary measurements
- Tracing line connects a pair of boundary points.

Formulation based on Petrou–Giannakidis idea

$2D$ continuous square domain $\rightarrow N \times N$ grid.
Recovery of $2D$ vector field in each tile $\rightarrow 2N^2$ unknowns.

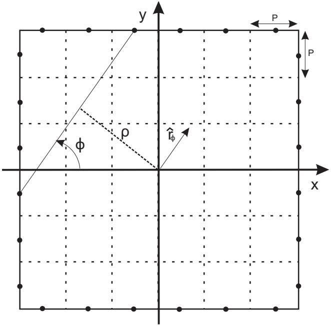

- $4N$ boundary measurements
- Tracing line connects a pair of boundary points.
- $6N^2$ numerical *model equations*.
  LS system

$$\boxed{\mathbf{b} = \bar{\mathbf{A}}\bar{\mathbf{x}}_{LS}}$$

Linear dependencies in *model equations*

Tracing lines $L_1, L_2 \ldots$ form closed curves.

Model equation can be expressed as a linear combination.

Linear dependencies in *model equations*

Tracing lines $L_1, L_2 \ldots$ form closed curves.

Model equation can be expressed as a linear combination.

recall $\int_{Closed-Path} \mathbf{E} dc = 0$

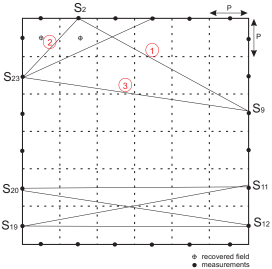

$$\int_{L_1} \mathbf{E} \cdot d\mathbf{r} + \int_{L_2} \mathbf{E} \cdot d\mathbf{r} + \int_{L_3} \mathbf{E} \cdot d\mathbf{r} = 0$$

Number of independent equations

For $4N$ points (sensors) along the boundaries, the maximum number of tracing lines to avoid loops is $4(N-1)$.

Number of independent equations

For $4N$ points (sensors) along the boundaries, the maximum number of tracing lines to avoid loops is $4(N-1)$.

The number of independent continuous model equations is $4(N-1)$

Independent equations in discrete domain

The problem is solved in the discrete domain. Thus,

Independent equations in discrete domain

The problem is solved in the discrete domain. Thus,

- Discretization and sampling errors are introduced in approximated *model equations*.

Independent equations in discrete domain

The problem is solved in the discrete domain. Thus,

- Discretization and sampling errors are introduced in approximated *model equations*.
- The summation of any set of the approximated equations cannot be zero in any closed path.

Independent equations in discrete domain

The problem is solved in the discrete domain. Thus,

- Discretization and sampling errors are introduced in approximated *model equations*.
- The summation of any set of the approximated equations cannot be zero in any closed path.
- No linear dependencies between equations.

Independent equations in discrete domain

The problem is solved in the discrete domain. Thus,

- Discretization and sampling errors are introduced in approximated *model equations*.
- The summation of any set of the approximated equations cannot be zero in any closed path.
- No linear dependencies between equations.
- matrix $\bar{\mathbf{A}}$ of $\mathbf{b} = \bar{\mathbf{A}}\bar{\mathbf{x}}_{LS}$ has full rank and condition number $k(\bar{\mathbf{A}}) < \infty$.

Continuous ill posed problem

Spatial resolution $N \to \infty$ i.e refinement of grid $N \times N$
Number of linearly independent equations $F(N) \to 4(N-1)$.

Continuous ill posed problem

Spatial resolution $N \to \infty$ i.e refinement of grid $N \times N$
Number of linearly independent equations $F(N) \to 4(N-1)$.

The number of independent equations cannot exceed the number of unknowns $2N^2$ as $N \to \infty$.

$$\lim_{N \to \infty} \frac{F(N)}{2N^2} = \lim_{N \to \infty} \frac{4(N-1)}{2N^2} = 0$$

Continuous ill posed problem

Spatial resolution $N \to \infty$ i.e refinement of grid $N \times N$
Number of linearly independent equations $F(N) \to 4(N-1)$.

The number of independent equations cannot exceed the number of unknowns $2N^2$ as $N \to \infty$.

$$\lim_{N\to\infty} \frac{F(N)}{2N^2} = \lim_{N\to\infty} \frac{4(N-1)}{2N^2} = 0$$

System $\mathbf{b} = \bar{\mathbf{A}}\bar{\mathbf{x}}_{LS}$ becomes unstable.

Continuous ill posed problem

Spatial resolution $N \to \infty$ i.e refinement of grid $N \times N$
Number of linearly independent equations $F(N) \to 4(N-1)$.

The number of independent equations cannot exceed the number of unknowns $2N^2$ as $N \to \infty$.

$$\lim_{N\to\infty} \frac{F(N)}{2N^2} = \lim_{N\to\infty} \frac{4(N-1)}{2N^2} = 0$$

System $\mathbf{b} = \bar{\mathbf{A}}\bar{\mathbf{x}}_{LS}$ becomes unstable.

3^{rd} Hadamard's criterion for well posedness is not satisfied

Numerical solution error

The solution depends on the discretization error (spatial resolution).

Numerical solution error

The solution depends on the discretization error (spatial resolution).

If spatial resolution N is finite it is proven that the relative error (RE)

$$\frac{\|\mathbf{x}_{exact} - \bar{\mathbf{x}}_{LS}\|}{\|\mathbf{x}_{exact}\|} \leq \frac{e_b}{1 - e_b} k(\mathbf{A}) < \infty$$

is bounded.

Numerical solution error

The solution depends on the discretization error (spatial resolution).

If spatial resolution N is finite it is proven that the relative error (RE)

$$\frac{\|\mathbf{x}_{exact} - \bar{\mathbf{x}}_{LS}\|}{\|\mathbf{x}_{exact}\|} \leq \frac{e_b}{1 - e_b} k(\mathbf{A}) < \infty$$

is bounded.

Existence of error bound ensures stability of the linear system.

Solution accuracy vs stability

Spatial resolution influences the accuracy of the solution and stability of the system.

- Accuracy is achieved if we increase the spatial resolution as more vector frequency components can be recovered.

Solution accuracy vs stability

Spatial resolution influences the accuracy of the solution and stability of the system.

- Accuracy is achieved if we increase the spatial resolution as more vector frequency components can be recovered.
- However, increase in spatial resolution deteriorates the conditioning (stability) of the system (high condition number).

Solution accuracy vs stability

Spatial resolution influences the accuracy of the solution and stability of the system.

- Accuracy is achieved if we increase the spatial resolution as more vector frequency components can be recovered.
- However, increase in spatial resolution deteriorates the conditioning (stability) of the system (high condition number).
- Stability of the system is important especially in the present of additive noise in input measurements. if there is no external sources of error then high condition number causes only a loss of digits accuracy in solution.

Stability indicators

- Singular values applying SVD in $\bar{\mathbf{A}}$ $\rightarrow$ Rapidly decreasing to zero $\Rightarrow$ increase of instability

Stability indicators

- Singular values applying SVD in $\bar{\mathbf{A}}$ $\rightarrow$ Rapidly decreasing to zero $\Rightarrow$ increase of instability
- Condition number k of $\bar{\mathbf{A}}$ $\rightarrow$ transfer error from matrix $\bar{\mathbf{A}}$ and vector $\mathbf{b}$ to the solution $\mathbf{x}$.

Stability indicators

- Singular values applying SVD in $\bar{\mathbf{A}}$ $\rightarrow$ Rapidly decreasing to zero $\Rightarrow$ increase of instability
- Condition number k of $\bar{\mathbf{A}}$ $\rightarrow$ transfer error from matrix $\bar{\mathbf{A}}$ and vector $\mathbf{b}$ to the solution $\mathbf{x}$.

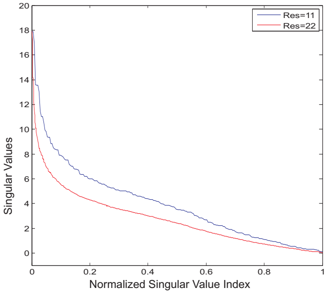

Condition Numbers:
$k_{Res=22} = 10^4$ and $k_{Res=11} = 174$

Recovered field for Res=11

$RE_{magnitude} = 0.11$ and $RE_{phase} = 0.05$

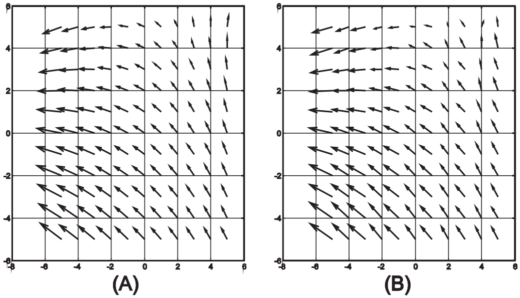

Recovered field for Res=22

$RE_{magnitude} = 0.08$ and $RE_{phase} = 0.045$

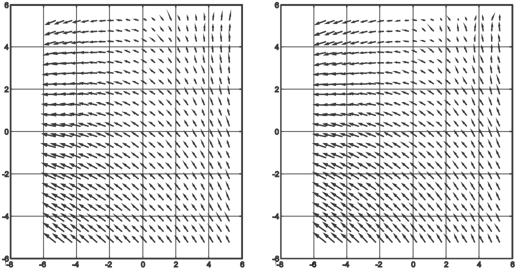

(A) (B)

Satisfactory conclusions

- We showed that the recovery of an irrotational field using direct numerical methods is possible.

Satisfactory conclusions

- We showed that the recovery of an irrotational field using direct numerical methods is possible.
- Discretization is a way to regularize this continuous ill posed problem and ensures a finite solution error bound.

Satisfactory conclusions

- We showed that the recovery of an irrotational field using direct numerical methods is possible.
- Discretization is a way to regularize this continuous ill posed problem and ensures a finite solution error bound.
- Next step is the practical aspects of the method:

Satisfactory conclusions

- We showed that the recovery of an irrotational field using direct numerical methods is possible.
- Discretization is a way to regularize this continuous ill posed problem and ensures a finite solution error bound.
- Next step is the practical aspects of the method:
  Inverse bioelectric field problem can be formulated using the proposed method.

Inverse bioelectric field problem

Estimation of the strengths and locations of the electric sources inside the brain or heart using partial differential equation (PDE) formulation and EEG or ECG recordings.
This is a very complicated task as there is difficulty in sources' formulation.

Inverse bioelectric field problem

Estimation of the strengths and locations of the electric sources inside the brain or heart using partial differential equation (PDE) formulation and EEG or ECG recordings.

This is a very complicated task as there is difficulty in sources' formulation.

Actually it is an ill posed problem as the same boundary recordings can be produced by different source distributions.

Comparison with PDE method

- No need of any prior information about the sources' formulation.

Comparison with PDE method

- No need of any prior information about the sources' formulation.
- The boundary conditions are directly incorporated in the line integral formulation.

Future Plan

- Optimal discretization of the bounded domain such as to balance the solution approximation error and the stability of the numerical system.

Future Plan

- Optimal discretization of the bounded domain such as to balance the solution approximation error and the stability of the numerical system.
- Arbitrary shapes of the bounded domain, more sophisticated numerical methods and additive noise in input measurements.

Future Plan

- Optimal discretization of the bounded domain such as to balance the solution approximation error and the stability of the numerical system.
- Arbitrary shapes of the bounded domain, more sophisticated numerical methods and additive noise in input measurements.
- Estimation of sources' locations as places where field has maxima or minima may indicate possible sources' locations.

Future Plan

- Optimal discretization of the bounded domain such as to balance the solution approximation error and the stability of the numerical system.
- Arbitrary shapes of the bounded domain, more sophisticated numerical methods and additive noise in input measurements.
- Estimation of sources' locations as places where field has maxima or minima may indicate possible sources' locations.
- Real bioelectric fields estimations using EEG recording and further comparisons with PDE method.